



**HAL**  
open science

## Abnormal spatial diffusion of Ca<sup>2+</sup> in F508del-CFTR airway epithelial cells

Fabrice Antigny, Caroline Norez, Anne Cantereau, Frédéric Becq, Clarisse  
Vandebrouck

► **To cite this version:**

Fabrice Antigny, Caroline Norez, Anne Cantereau, Frédéric Becq, Clarisse Vandebrouck. Abnormal spatial diffusion of Ca<sup>2+</sup> in F508del-CFTR airway epithelial cells. *Respiratory Research*, 2008, 9 (1), pp.70. 10.1186/1465-9921-9-70 . hal-03119859

**HAL Id: hal-03119859**

**<https://hal.science/hal-03119859v1>**

Submitted on 25 Jan 2021

**HAL** is a multi-disciplinary open access archive for the deposit and dissemination of scientific research documents, whether they are published or not. The documents may come from teaching and research institutions in France or abroad, or from public or private research centers.

L'archive ouverte pluridisciplinaire **HAL**, est destinée au dépôt et à la diffusion de documents scientifiques de niveau recherche, publiés ou non, émanant des établissements d'enseignement et de recherche français ou étrangers, des laboratoires publics ou privés.

Research

Open Access

## Abnormal spatial diffusion of $\text{Ca}^{2+}$ in F508del-CFTR airway epithelial cells

Fabrice Antigny, Caroline Norez, Anne Cantereau, Frédéric Becq and Clarisse Vandebrouck\*

Address: Institut de Physiologie et Biologie Cellulaires, Université de Poitiers, CNRS, 86022 Poitiers, France

Email: Fabrice Antigny - [fabrice.antigny@etu.univ-poitiers.fr](mailto:fabrice.antigny@etu.univ-poitiers.fr); Caroline Norez - [caroline.norez@univ-poitiers.fr](mailto:caroline.norez@univ-poitiers.fr);

Anne Cantereau - [anne.cantereau@univ-poitiers.fr](mailto:anne.cantereau@univ-poitiers.fr); Frédéric Becq - [frederic.becq@univ-poitiers.fr](mailto:frederic.becq@univ-poitiers.fr);

Clarisse Vandebrouck\* - [clarisse.vandebrouck@univ-poitiers.fr](mailto:clarisse.vandebrouck@univ-poitiers.fr)

\* Corresponding author

Published: 30 October 2008

Received: 1 April 2008

*Respiratory Research* 2008, **9**:70 doi:10.1186/1465-9921-9-70

Accepted: 30 October 2008

This article is available from: <http://respiratory-research.com/content/9/1/70>

© 2008 Antigny et al; licensee BioMed Central Ltd.

This is an Open Access article distributed under the terms of the Creative Commons Attribution License (<http://creativecommons.org/licenses/by/2.0>), which permits unrestricted use, distribution, and reproduction in any medium, provided the original work is properly cited.

### Abstract

**Background:** In airway epithelial cells, calcium mobilization can be elicited by selective autocrine and/or paracrine activation of apical or basolateral membrane heterotrimeric G protein-coupled receptors linked to phospholipase C (PLC) stimulation, which generates inositol 1,4,5-trisphosphate ( $\text{IP}_3$ ) and 1,2-diacylglycerol (DAG) and induces  $\text{Ca}^{2+}$  release from endoplasmic reticulum (ER) stores.

**Methods:** In the present study, we monitored the cytosolic  $\text{Ca}^{2+}$  transients using the UV light photolysis technique to uncage caged  $\text{Ca}^{2+}$  or caged  $\text{IP}_3$  into the cytosol of loaded airway epithelial cells of cystic fibrosis (CF) and non-CF origin. We compared in these cells the types of  $\text{Ca}^{2+}$  receptors present in the ER, and measured their  $\text{Ca}^{2+}$  dependent activity before and after correction of F508del-CFTR abnormal trafficking either by low temperature or by the pharmacological corrector miglustat (N-butyldeoxyjirimycin).

**Results:** We showed reduction of the inositol 1,4,5-trisphosphate receptors ( $\text{IP}_3\text{R}$ ) dependent- $\text{Ca}^{2+}$  response following both correcting treatments compared to uncorrected cells in such a way that  $\text{Ca}^{2+}$  responses (CF+treatment vs wild-type cells) were normalized. This normalization of the  $\text{Ca}^{2+}$  rate does not affect the activity of  $\text{Ca}^{2+}$ -dependent chloride channel in miglustat-treated CF cells. Using two inhibitors of  $\text{IP}_3\text{R}$ , we observed a decrease of the implication of  $\text{IP}_3\text{R}$  in the  $\text{Ca}^{2+}$  response in CF corrected cells. We observed a similar  $\text{Ca}^{2+}$  mobilization between CF-KM4 cells and CFTR-cDNA transfected CF cells (CF-KM4-reverted). When we restored the F508del-CFTR trafficking in CFTR-reverted cells, the specific  $\text{IP}_3\text{R}$  activity was also reduced to a similar level as in non CF cells. At the structural level, the ER morphology of CF cells was highly condensed around the nucleus while in non CF cells or corrected CF cells the ER was extended at the totality of cell.

**Conclusion:** These results suggest reversal of the  $\text{IP}_3\text{R}$  dysfunction in F508del-CFTR epithelial cells by correction of the abnormal trafficking of F508del-CFTR in cystic fibrosis cells. Moreover, using CFTR cDNA-transfected CF cells, we demonstrated that abnormal increase of  $\text{IP}_3\text{R}$   $\text{Ca}^{2+}$  release in CF human epithelial cells could be the consequence of F508del-CFTR retention in ER compartment.

## Introduction

The existence of distinct membrane localizations and multiple isoforms of inositol 1,4,5-trisphosphate (IP<sub>3</sub>) receptors (IP<sub>3</sub>R) within the same cell type may explain the complex spatiotemporal patterns of Ca<sup>2+</sup> release from IP<sub>3</sub>-sensitive calcium pools in epithelial cells. In addition to requiring IP<sub>3</sub>, IP<sub>3</sub>R are regulated in a biphasic manner by direct interaction with Ca<sup>2+</sup>, *i.e.* activation at low concentrations (up to 0.3 μM) and inhibition at higher concentrations (0.5–1 μM) [1]. The different modes of interaction of IP<sub>3</sub>R with Ca<sup>2+</sup> are involved in the complex feedback regulation of the Ca<sup>2+</sup> release [2]. IP<sub>3</sub>R activity is also regulated by Ca<sup>2+</sup>-independent accessory proteins, Mg<sup>2+</sup>, redox potential and ATP [3]. Furthermore, a local Ca<sup>2+</sup> discharge by photolysis of NP-EGTA technique can activate the IP<sub>3</sub>R Ca<sup>2+</sup> release. For example, the type 3 IP<sub>3</sub>R remaining open in the presence of high Ca<sup>2+</sup> concentration, initiates a rapid, large and almost total release of Ca<sup>2+</sup> from intracellular stores [4]. These properties place IP<sub>3</sub>R at the heart of calcium signalling pathways.

Recent studies have demonstrated higher intracellular Ca<sup>2+</sup> mobilization in Cystic Fibrosis (CF) compared to normal human nasal [5] or bronchial [6] epithelia. Cystic Fibrosis is the most frequent lethal autosomal recessive genetic disease in Caucasian population. The most common mutation in CF is a deletion of phenylalanine at position 508 in the Cystic Fibrosis Transmembrane conductance Regulator protein (F508del-CFTR). F508del-CFTR protein is misfolded, trapped in the endoplasmic reticulum (ER) by the ER quality control (ERQC) [7] and subsequently submitted to proteasomal degradation [8].

In this report we monitored the cytosolic Ca<sup>2+</sup> transients using the flash photolysis technique to uncage caged Ca<sup>2+</sup> into the cytosol of nitrophenyl-EGTA (NP-EGTA) loaded human CF nasal epithelial CF15 cells [9], human CF tracheal gland CF-KM4 cells [10] and human non-CF tracheal gland epithelial MM39 cells [11]. We also used the membrane-permeable UV light photolysis caged IP<sub>3</sub> analogue (iso-Ins(1,4,5)P<sub>3</sub>/PM) to examine the consequence on the local IP<sub>3</sub>R Ca<sup>2+</sup> release of rescuing F508del-CFTR by the pharmacological corrector miglustat [12] and after culturing cells at low temperature [13].

## Materials and methods

### Cells

Human nasal epithelial JME/CF15 cells (F508del/F508del) were grown at 37°C in 5% CO<sub>2</sub> under standard culture conditions [9]. Human CF and non-CF tracheal gland serous CF-KM4 and MM39 cells were cultured as previously described [5]. The CF-KM4 cells transduced with the lentiviral vector expressing the wild-type CFTR cDNA [14] (named in this study CF-KM4 reverted), were generously given by Dr. Christelle Coraux (INSERM U514, Reims University, IFR53, Reims, France).

### Extraction of IP<sub>3</sub>R mRNA and reverse transcription

Total RNA was extracted using RNABle® (Eurobio), according to the protocol provided by the manufacturer and mRNA was reverse transcribed to cDNA as described elsewhere [15]. The specific oligonucleotide primers used for each subtype of the IP<sub>3</sub>R are presented Table 1. The temperature cycling conditions were initial melting at 94°C for 5 min, annealing at 56°C for 2 min followed by 30 cycles of 72°C for 30 s, 94°C for 30 s, annealing of 56°C for 30 s and a final extension at 72°C for 5 min.

### Quantification of IP<sub>3</sub>R mRNA by RT-PCR

Quantitative PCR was used to determine the copy numbers of IP<sub>3</sub>R1, IP<sub>3</sub>R2, and IP<sub>3</sub>R3 in mRNA extracted from CF15 cells in different conditions. The IP<sub>3</sub>R mRNA quantities were normalized against β-actin. Quantitative PCR were performed on the ABI Prism 7700. The specific oligonucleotide primer used for each subtype of the IP<sub>3</sub>R is presented Table 1. For β-actin-cDNA, the primers were 5'-TGTGGATCGGCGGCTC-3' and 5'-ACTCCTGCTTGCTGCTGATCCAT-3' (900 nM for each primer). The probe taqman FAM used was 5'-FAM-TGGCCTCGCTGTCCACCTTCCA-TAMRA3' (200 nM). The temperature cycling conditions were: initial melting at 94°C for 5 min, annealing at 56°C for 2 min followed by 30 cycles of 72°C for 30 s, 94°C for 30 s, annealing of 56°C for 30 s and a final extension at 72°C for 30 s. Each sample was analysed in triplicate. After PCR was completed, the FAM fluorescent signal (490 nm) was analysed and converted into a relative number of copies of target molecules. These results were expressed by threshold cycle value (Ct = number of necessary amplification cycle that emitted the fluorescent signal superior at non specific fluorescence).

**Table 1: Specific primers for each IP<sub>3</sub>R subtype**

	Accession number	Primer sens	Primer anti-sens	bp
hIITPR 1	NM_002222	5'-AACCGCTACTC TGCCCAAAA-3'	5'AGTTTGTTGAGTAGCACTGCGTCT-3'	86
hIITPR 2	NM_002223	5'-GCGATCTGCA CATCTATGCTG-3'	5'-AAGTATTAATGTA GGCCCAAGACCTATT-3'	117
hIITPR 3	NM_002224	5'-GGGCTCTCG GTGCCTGA-3'	5'-GGAGGGCTTGC GGAGAA-3'	150

### Immunofluorescence

Cells were incubated with a primary specific antibody. We used the following primary specific antibody for each IP<sub>3</sub>R isoform: rabbit anti-IP<sub>3</sub>R1 polyclonal antibody (1:1000, Affinity Bioreagents), goat anti-IP<sub>3</sub>R2 polyclonal antibody (1:1000, Santa Cruz Biotechnology), mouse anti-IP<sub>3</sub>R3 monoclonal antibody (1:1000, Santa Cruz Biotechnology) and the rabbit anti-calreticulin antibody (1:100, Stressgen Biotechnologies) for 1 h at room temperature. Cells were then incubated with the corresponding conjugated antibody. In the control, the primary antibody was omitted. The nuclei were labelled with TOPRO-3 (1:1000, Interchim). Other details are as described [16].

### Imaging of endoplasmic reticulum

Cells were incubated in 0.5  $\mu$ M ER tracker (FluoProbes<sup>®</sup>) for 10 min at 37 °C. This probe was excited at 488 nm, and the emission (510 nm) was recorded with a spectral confocal station FV 1000 installed on an inverted microscope IX-81 (Olympus Tokyo, Japan).

### Functional assay

Ca<sup>2+</sup>-activated chloride channels activity was assayed on epithelial cell populations by the iodide (<sup>125</sup>I) efflux technique as described [12].

### Recording global calcium signals

Cells were loaded with 3  $\mu$ M Fluo-4 acetoxymethyl ester (FluoProbes<sup>®</sup>) for 20 min at room temperature and Ca<sup>2+</sup> activity was recorded by confocal laser scanning microscopy using Bio-Rad MRC 1024. All the experiments were performed at minimum on two different cell passages (2 < N < 5), and in each field various cells were selected. This number of cells is noted n on each histogram. Other details are as described [16].

### Monitoring cytosolic Ca<sup>2+</sup> transients induced by uncaging Ca<sup>2+</sup>

Cells were loaded with 3  $\mu$ M nitrophenyl-EGTA (NP-EGTA) (Interchim, Montluçon, France) [17] for 40 min, and 20 min with NP-EGTA plus 3  $\mu$ M Fluo-4 AM at room temperature in buffer solution containing: (in mM) 130 NaCl, 5.4 KCl, 2.5 CaCl<sub>2</sub>, 0.8 MgCl<sub>2</sub>, 5.6 glucose, 10 Hepes, pH 7.4 (adjusted with Tris base). Cells were then washed and allowed to desesterification for 10 min. Ca<sup>2+</sup> transients were monitored using confocal laser scanning microscope FV1000 (Olympus, France) installed on an inverted microscope IX-81 (Olympus, Tokyo, Japan) and equipped with two scanning heads. One is used for imaging Fluo-4 fluorescence with 488 nm line of a multi-line argon laser using line scan mode, the other allows stimulation (SIMS) with 405 nm diode. XT images were acquired with  $\times$ 60/1.2 NA water-immersion objective with 2 $\times$  optical zoom (spatial resolution of 0.2  $\mu$ m/pixel) and collected using spectral detector within 500–600 nm.

To allow comparison between different experimental conditions, uncaging pulses of the same intensity were delivered with 5% of 405 nm diode for 500 ms with tornado scanning mode in a region of interest of 10 pixels diameter (= 2  $\mu$ m). Simultaneous scanner system of Olympus FV1000 station allows laser stimulation in a restricted region while recording Fluo-4 fluorescence images with no delay and high resolution. As shown on XY images, laser stimulation with 405 nm diode applied on a restricted region of interest (yellow circle in Fig. 1A) induced a localized Ca<sup>2+</sup> increase that propagated throughout the cell. For high time resolution, intracellular Ca<sup>2+</sup> images were acquired in a line scan mode during 3 s (XT image, Fig. 1B) with line scan defined in the center of stimulation region (XY reference image, Fig. 1A). 500 ms duration of laser stimulation was chosen for its efficacy to induce large response with no sign of bleach or saturation of cellular response. Typical intensity profile of Ca<sup>2+</sup> variation was then extracted from XT images with FV10-ASW v1.3 software within a 10 pixels width region to reduce noise (Fig. 1C). Intensity profiles were normalized by dividing the fluorescence intensity of each pixel (F) by the average resting value before stimulation (F<sub>0</sub>) to generate an (F-F<sub>0</sub>/F<sub>0</sub>) image. With this intensity profile, we compared the different Ca<sup>2+</sup> responses by measuring the area under the curve (AUC) and the peak value (Fig. 1C).

### Caged IP<sub>3</sub> experiments

To activate directly the IP<sub>3</sub>Rs we used the membrane-permeable UV light-sensitive caged IP<sub>3</sub> analogue, [D-2,3-O-Isopropylidene-6-O-(2-nitro-4,5-dimethoxy)benzyl-myo-inositol 1,4,5-trisphosphate-hexakis(propionoxymethyl)ester] = iso-Ins(1,4,5)P<sub>3</sub>/PM. Cells were loaded with 1.5  $\mu$ M iso-Ins(1,4,5)P<sub>3</sub>/PM (Alexis Biochemicals) [17] for 45 min, and still 20 min with iso-Ins(1,4,5)P<sub>3</sub>/PM plus 3  $\mu$ M Fluo-4 AM at room temperature in buffer solution containing: (in mM) 130 NaCl, 5.4 KCl, 2.5 CaCl<sub>2</sub>, 0.8 MgCl<sub>2</sub>, 5.6 glucose, 10 Hepes, pH 7.4 (adjusted with Tris base). Cells were then washed and allowed to desesterification for 20 min. Ca<sup>2+</sup> transients were monitored using a confocal laser scanning microscope FV1000 (Olympus, France) in absence of extracellular Ca<sup>2+</sup>. To allow comparison between different experimental conditions, uncaging pulses of the same intensity were delivered with 8% of 405 nm diode for 100 ms with tornado scanning mode in a region of interest of 10 pixels diameter (= 2  $\mu$ m). Simultaneous scanner system of Olympus FV1000 station allows laser stimulation in a restricted region while recording Fluo-4 fluorescence images with no delay and high resolution. Experiments were conducted at room temperature. Intensity profiles were normalized by dividing the fluorescence intensity of each pixel (F) by the average resting value before stimulation (F<sub>0</sub>) to generate an (F-F<sub>0</sub>/F<sub>0</sub>) image. With this intensity

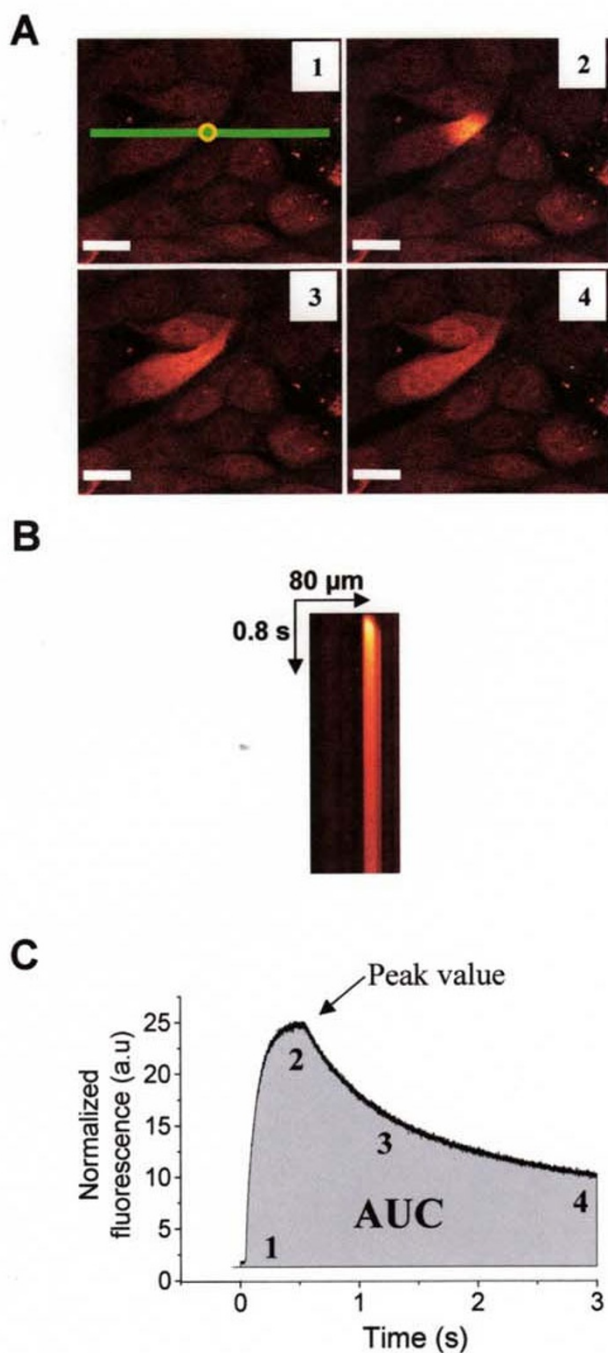


**Figure 1**

profile, we compared the different  $\text{Ca}^{2+}$  responses by measuring the area under the curve (AUC).

#### Statistics

Results are expressed as mean  $\pm$  SEM of  $n$  observations. Sets of data were compared with a Student's  $t$  test. Differences were considered statistically significant when  $P <$

#### Figure 1

**Determination of localized  $\text{Ca}^{2+}$  mobilization by  $\text{Ca}^{2+}$  caged technique.** A Confocal XY images illustrating  $\text{Ca}^{2+}$  release by photolysis of NP-EGTA molecule. The uncaging pulses were delivered with 5% of 405 nm diode for 500 ms with tornado scanning mode in a region of interest of 10 pixels diameter (yellow circle). Scale bars 25  $\mu\text{m}$ . B XT images were obtained by acquisition in line scan mode (green line in A) during 3 s. C Typical intensity profile of  $\text{Ca}^{2+}$  variation was extracted from XT images presented in B, the grey area represents the measure of area under the curve (AUC). The number 1 to 4 represented the  $\text{Ca}^{2+}$  response induce by the photolysis at different time (in figure 1A and 1C). All the parameters automatically measured with a computer program developed in our laboratory under IDL 5.3 structured language were represented on the typical intensity profile (peak and kinetics parameters).

0.05. ns: non significant difference, \*  $P < 0.05$ , \*\*  $P < 0.01$ , \*\*\*  $P < 0.001$ . All statistical tests were performed using GraphPad Prism version 4.0 for Windows (Graphpad Software) and Origin version 5.0.

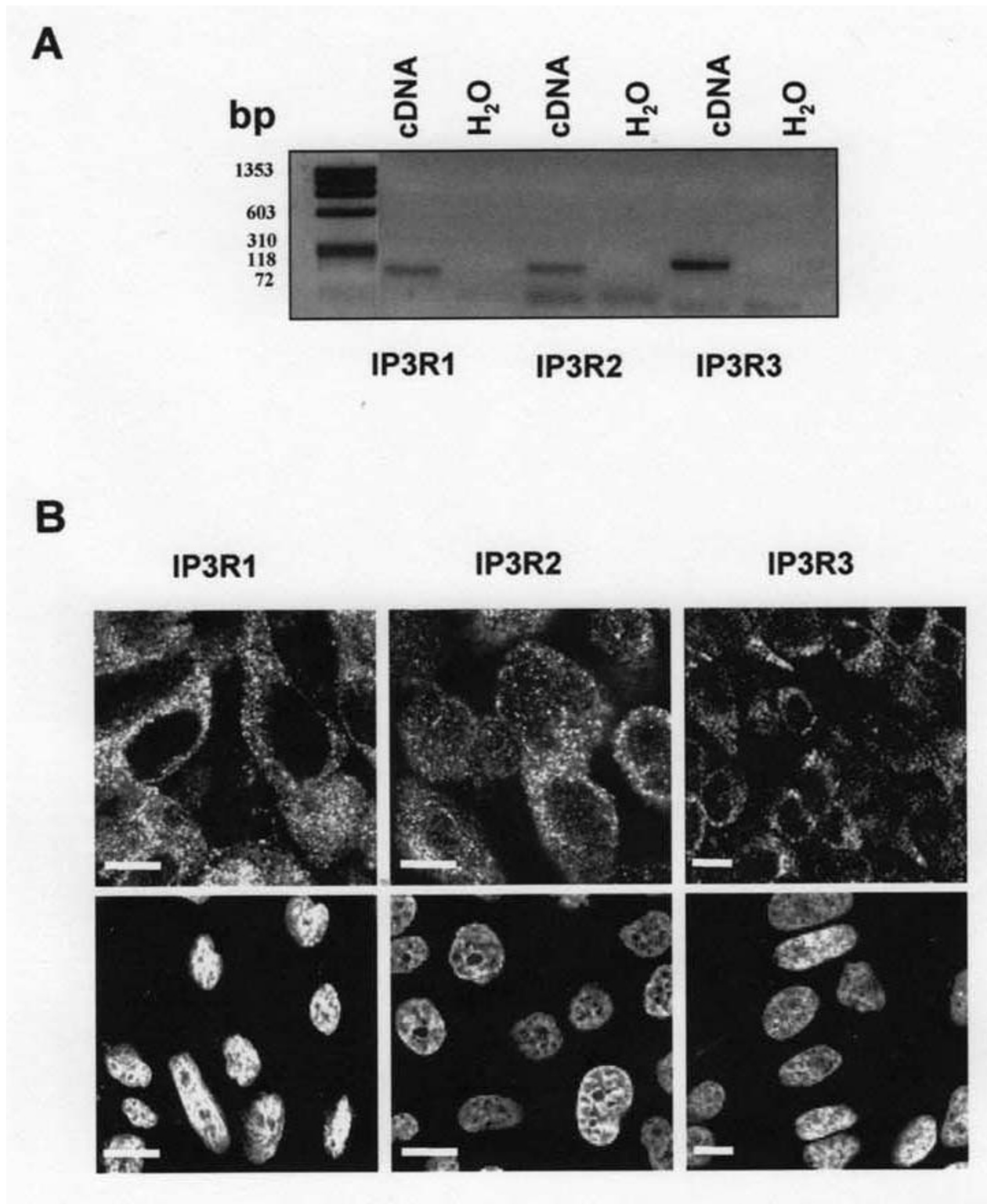
#### Chemicals

2-APB, decavanadate, cyclosporine A, histamine, ATP, A23187 and Caffeine are from Sigma. Thapsigargin is from LC Laboratories. Miglustat and NB-DGJ are from Toronto Research Chemicals.

#### Results

##### Role of $\text{IP}_3$ receptors in local ER $\text{Ca}^{2+}$ mobilization in human epithelial cells

We first characterized  $\text{IP}_3\text{R}$  isoforms in human nasal epithelial CF15 cells. Using reverse transcription-PCR technique, we found mRNA for the three isoforms of  $\text{IP}_3\text{R}$  (Fig. 2A). Moreover, confocal immunofluorescence microscopy studies of  $\text{IP}_3\text{Rs}$  indicated for each isoform a punctiform and diffuse immunostaining in the cytoplasm of CF15 cells (Fig. 2B top images). No immunostaining of  $\text{IP}_3\text{Rs}$  was detected when the primary antibodies were omitted (Fig. 2B bottom images). Then, to directly investigate  $\text{IP}_3\text{R}$  activity, we used the flash photolysis technique to uncage caged  $\text{Ca}^{2+}$  into the cytosol of NP-EGTA loaded CF15 cells [17]. Because the capacity of  $\text{IP}_3$  receptors to release  $\text{Ca}^{2+}$  into the cytosol is influenced, in part, by the cytosolic local  $\text{Ca}^{2+}$  concentration, a confined discharge of  $\text{Ca}^{2+}$  by NP-EGTA photolysis induced an activation of  $\text{Ca}^{2+}$  release by  $\text{IP}_3$  receptors. To eliminate  $\text{Ca}^{2+}$  influx, we performed all experiments in absence of extracellular  $\text{Ca}^{2+}$  ( $\text{Ca}^{2+}$ -free). As described in the method section, images were acquired in a line scan mode during 3 s (XT image) with CF15 cells cultured at 37°C (Fig. 3A). The corresponding normalized fluorescence and AUC are shown Fig. 3B (black line) and C (black bar). To study the contri-

**Figure 2**

**Characterization of IP<sub>3</sub>R isoforms in human nasal epithelial cells.** A mRNA amplification of 3 isoforms of IP<sub>3</sub>R by real time PCR. B Immunostaining of IP<sub>3</sub>R type 1, 2 and 3 in untreated CF15 cells and staining with the secondary antibody as a negative control (bottom panels); nuclei are labelled with TOPRO-3, bar = 10 μm.

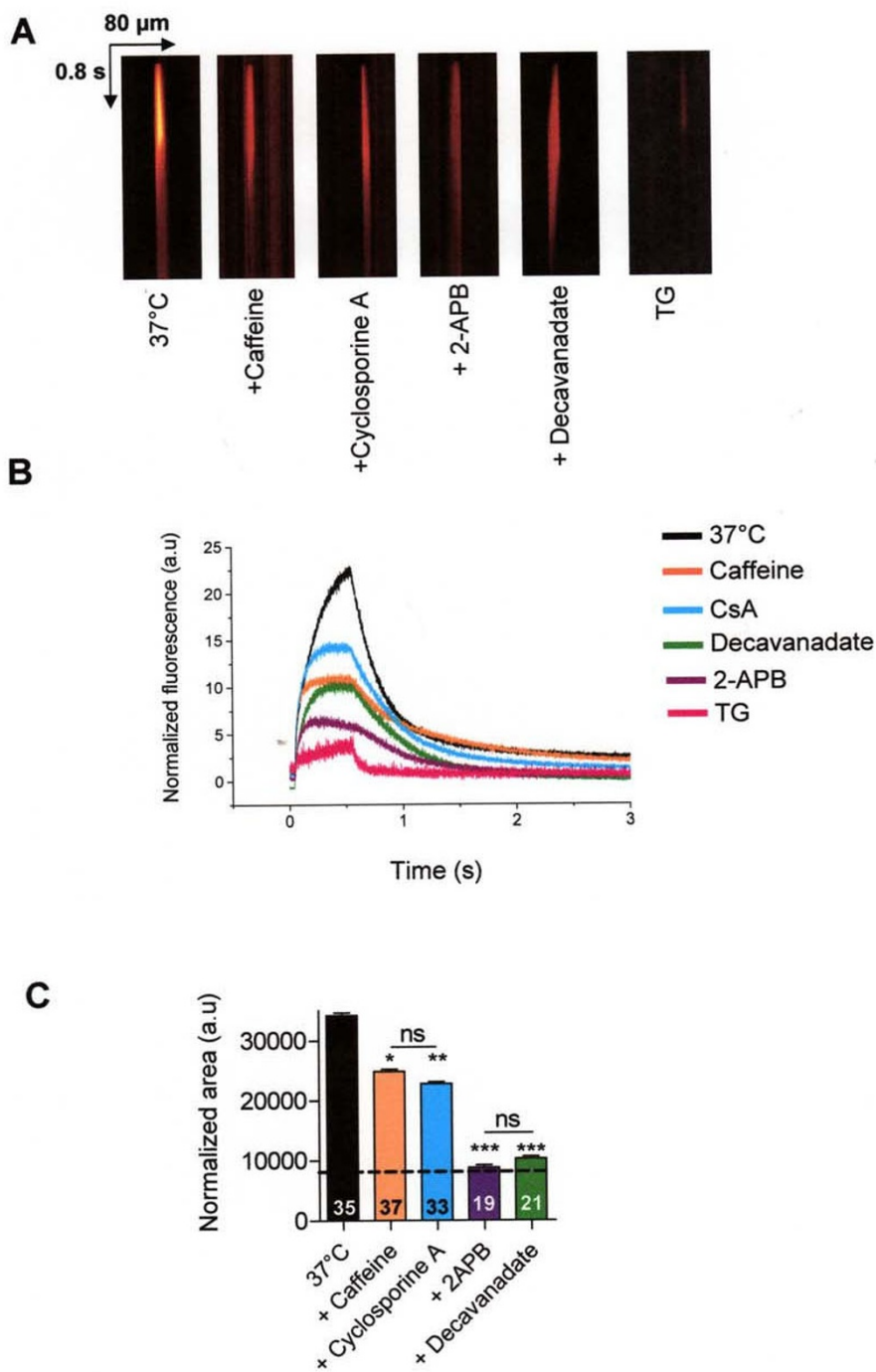


**Figure 3**

**Pharmacology of IP<sub>3</sub>R response of local uncaging of caged Ca<sup>2+</sup> in CF15 cells in absence of extracellular Ca<sup>2+</sup>.** *A* Example of line-scan images acquired at 2 ms per line and 0.21  $\mu$ m per pixel in CF15 cells untreated at 37°C in presence or not of 100  $\mu$ M 2-APB, 100  $\mu$ M decavanadate, 20 mM caffeine or 10  $\mu$ M cyclosporine A (all were preincubated during 10 min) and after 2 h incubation with 10  $\mu$ M thapsigargin (TG). *B* Average of the line-scan images in *A* expressed as normalized fluorescence in each conditions *C* Mean normalized area measured from XT images in each experimental condition. The dash line represents the response induced by the flash only, after complete ER Ca<sup>2+</sup> store depletion. Results are presented as mean  $\pm$  SEM and the number of experiments is noted on each bar graph. \* P < 0.05; \*\* P < 0.01; \*\*\* P < 0.001; ns, non significant difference.

bution of IP<sub>3</sub> receptors into the local Ca<sup>2+</sup> release in CF15 cells, we used 2-APB and decavanadate [18], two non specific inhibitors of IP<sub>3</sub>R isoforms. In these experimental conditions, we observed a decrease by more than 70% of the Ca<sup>2+</sup> response when we used either 100 μM 2-APB or 100 μM decavanadate (Fig. 3A–C). To prevent the release of Ca<sup>2+</sup> by IP<sub>3</sub>Rs from the ER, we measured the response that had been only induced by the flash. We treated cells 2 h with 10 μM thapsigargin (TG) to release the whole Ca<sup>2+</sup> store. The light stimulation in presence of TG produced a very small response corresponding only to ~20% of the response obtained at 37 °C (Fig. 3A–B). In presence of the receptor blockers, these Ca<sup>2+</sup> responses were similar to the response induced only by the photolysis flash (represented in Fig. 3C by a dashed black line). These experiments demonstrate that the total Ca<sup>2+</sup> response in human nasal epithelial CF15 cells is due to the activity of IP<sub>3</sub> receptors.

To discriminate between the different isoforms of IP<sub>3</sub>Rs implicated in Ca<sup>2+</sup> release, we used two inhibitors of IP<sub>3</sub>R1 (caffeine, cyclosporine A) in absence of extracellular Ca<sup>2+</sup> (Fig. 3). Caffeine is known to inhibit the IP<sub>3</sub>R type 1 and to inhibit this isoform at millimolar concentrations [19]. In our hand, 20 mM caffeine induced an inhibition of Ca<sup>2+</sup> response limited to the peak intensity (Fig. 3B). The Ca<sup>2+</sup> quantity mobilized in presence of caffeine decreased by 30% (Fig. 3C). We also compared the uncaged Ca<sup>2+</sup> response induced by UV flash photolysis in presence of cyclosporine A (CsA), an agent known to abolish type 1 IP<sub>3</sub>R [20]. Cyclosporine A induced a decrease of peak fluorescence intensity and a decrease of Ca<sup>2+</sup> quantity mobilization by 45% (Fig. 3B–C). Since, we have shown previously the absence of ryanodine receptors in human nasal epithelial cells line [5], the fraction of Ca<sup>2+</sup> response not inhibited by cyclosporine A or caffeine probably arose from the two other isoforms of IP<sub>3</sub>R (type 2 and 3) activity.

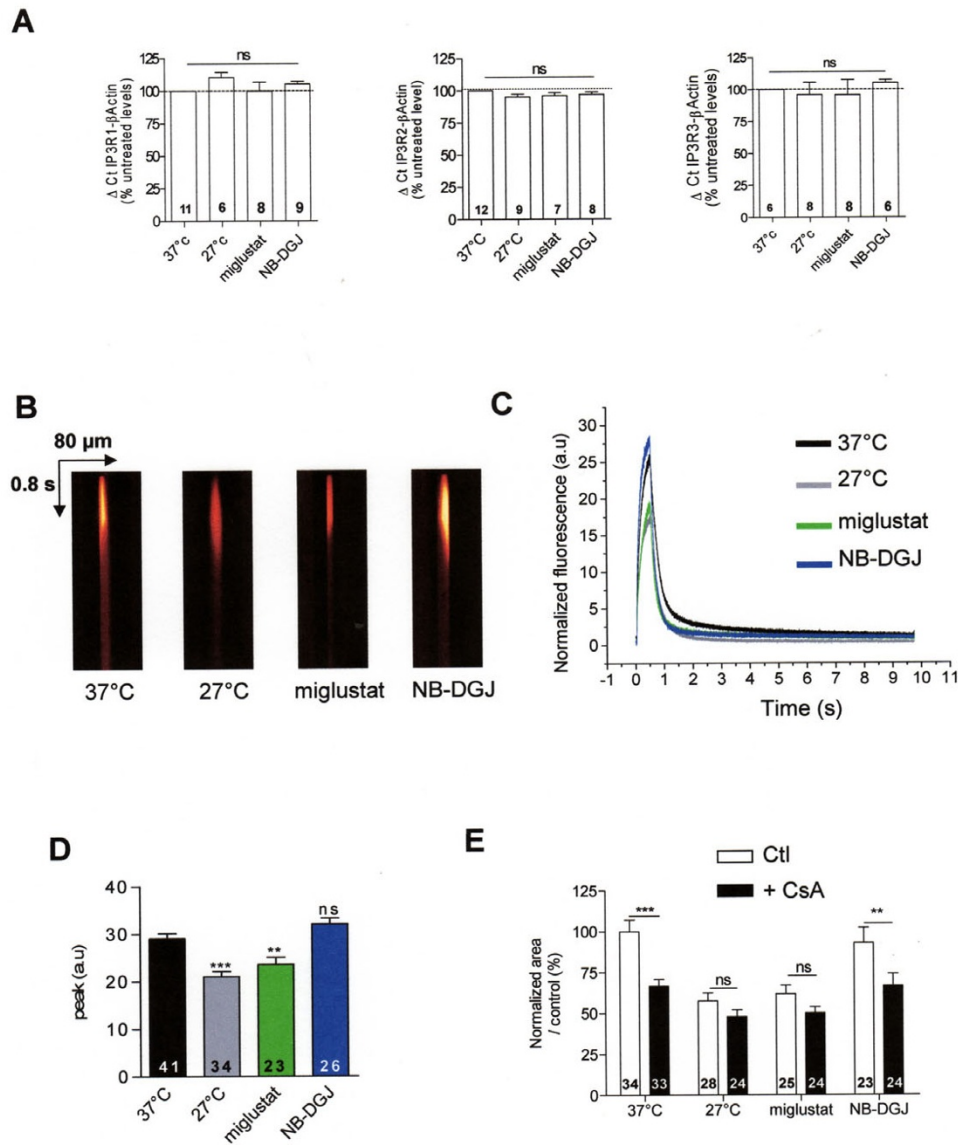
#### **Consequence on local IP<sub>3</sub>Rs Ca<sup>2+</sup> activity of rescuing F508del-CFTR in CF cells**

To study the consequence of F508del-CFTR rescue on the IP<sub>3</sub>R activity, before loading with NP-EGTA, CF15 cells were either cultured at 27 °C during 24 h or incubated 2 h with a culture medium containing 100 μM miglustat. We compared the mRNA quantity of each IP<sub>3</sub>R isoform by quantitative RT-PCR (Fig. 4A), and found no variation of mRNA for each IP<sub>3</sub>R isoforms whatever the experimental conditions (Fig. 4A). The activity of IP<sub>3</sub> receptors was then evaluated. Example of intracellular Ca<sup>2+</sup> XT images are provided for each experimental condition (Fig. 4B). By analysis of the XT images, we observed a decrease by ≈ 40% and 50% in temperature- (24 h at 27 °C, grey trace and bar) and miglustat-corrected CF15 cells (2 h at 100 μM, green trace and bar), respectively, compared to uncor-

rected CF15 cells (37 °C, black trace and bar) (Fig. 4C–D). We used NB-DGJ, because this compound is not able to rescue the abnormal trafficking of F508del-CFTR [16]. It is remarkable that treating CF15 cells with NB-DGJ (2 h at 100 μM) did not modify the Ca<sup>2+</sup> response compared to untreated CF15 cells as shown by the XT images (Fig. 4B) and the histograms (blue trace and bar Fig. 4C–D). Fig. 4D also provides the corresponding statistical analysis for all these experiments. Therefore, these results show that the rescue of F508del-CFTR either by miglustat or by low temperature deeply affects the capacity of the ER to release Ca<sup>2+</sup> into the cytosol of CF15 cells. In each treatment condition, IP<sub>3</sub>R1 inhibition by 10 μM CsA induced a significant decrease of Ca<sup>2+</sup> response by 40% in control or NB-DGJ treated cells (Fig. 4E). In contrast, 10 μM CsA did not modify the Ca<sup>2+</sup> response in CF15 corrected cells (low temperature or miglustat treatments) (Fig. 4E).

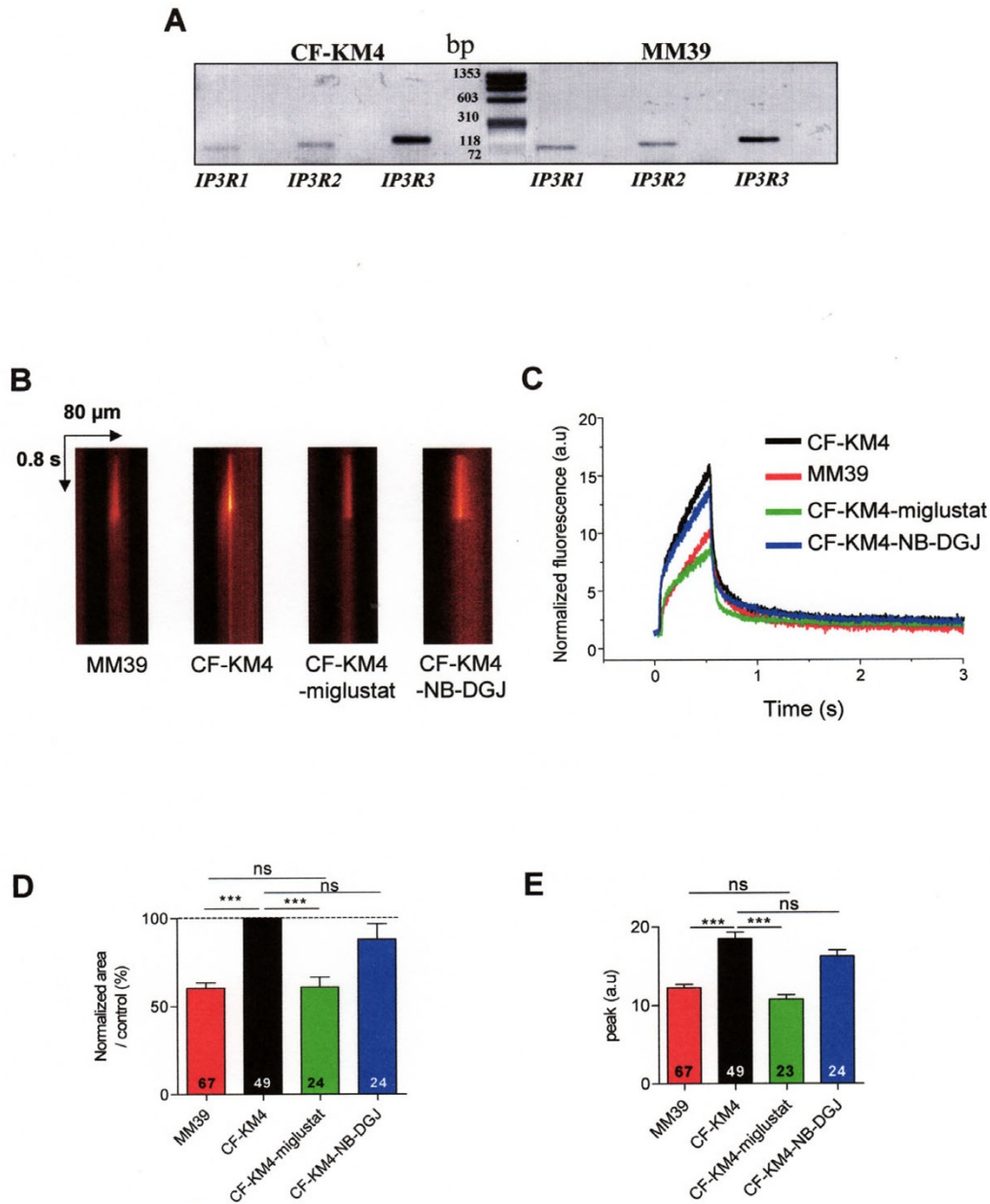
To complement this study and to confirm our results, we used two other epithelial cell lines which have another tissue origin: the human tracheal gland serous CF cells (CF-KM4) and non CF cells (MM39). As in CF15 cells, the RT-PCR technique shows the presence of IP<sub>3</sub>R1, IP<sub>3</sub>R2 and IP<sub>3</sub>R3 in both human tracheal CF-KM4 and MM39 cells (Fig. 5A). To confirm the exacerbated ER Ca<sup>2+</sup> release in CF cells, we also applied the NP-EGTA technique to examine IP<sub>3</sub>R Ca<sup>2+</sup> dependent activity in MM39 and CF-KM4 cells. The Ca<sup>2+</sup> responses (Fig. 5B–D) showed 40% increase of the Ca<sup>2+</sup> response in CF-KM4 cells *versus* non-CF MM39 cells (black and red traces and histograms, respectively). Figure 5B shows line-scan XT images recorded in the absence of extracellular Ca<sup>2+</sup> in MM39 cells and in CF-KM4 cells maintained either at 37 °C, or at 37 °C for 2 h in presence of miglustat or NB-DGJ. The Ca<sup>2+</sup> response in CF cells was decreased by ≈ 40% after miglustat treatment (Fig. 5B–E, green traces and histograms). The local Ca<sup>2+</sup> response obtained following miglustat treatment was similar to that obtained with the non-CF MM39 cells (Fig. 5C, red traces and histograms). As for CF15 cells, NB-DGJ did not induce any variation of Ca<sup>2+</sup> response in CF-KM4 cells compared to uncorrected CF-KM4 cells (Fig. 5D). In fact, the peak of the Ca<sup>2+</sup> responses was decreased in non CF MM39 cells and miglustat-corrected CF-KM4 cells compared to uncorrected CF-KM4 cells (Fig. 5C, E). Thus, correction of the abnormal F508del-CFTR trafficking by miglustat induces a profound modification of IP<sub>3</sub>R Ca<sup>2+</sup> dependent activity in CF cells.

Then, we measured the global ER Ca<sup>2+</sup> release (in absence of extracellular Ca<sup>2+</sup>) by 100 μM histamine in control or NB-DGJ treated CF-KM4 or corrected CF-KM4 (by low temperature or miglustat), and on untreated or miglustat-treated MM39 cells (Fig. 6A–B). These experiments show that the Ca<sup>2+</sup> response induced by histamine was decreased in CF-KM4 cells corrected either by temperature



**Figure 4**

**Modification of local stimulation of caged Ca<sup>2+</sup> in corrected F508del-CFTR CF15 cells.** **A** Relative mRNA expression level of IP<sub>3</sub>R-1, IP<sub>3</sub>R-2, and IP<sub>3</sub>R-3 in different conditions compared to βActin mRNA expression. **B** Example of line-scan images acquired at 2 ms per line and 0.21 μm per pixel in CF15 cells treated (27°C, miglustat, NB-DGJ) and uncorrected at 37°C in absence of extracellular Ca<sup>2+</sup>. **C** Average of the line-scan images in **B** expressed as normalized fluorescence in absence of extracellular Ca<sup>2+</sup>. **D** Histograms showing the amplitude of IP<sub>3</sub>R Ca<sup>2+</sup> response in various experimental conditions as indicated. **E** Mean normalized area in each experimental treatment in absence or presence of 10 μM CsA. Sets of data were compared to the control CF15. Results are presented as mean ± SEM and the number of experiments is noted on each bar graph. \*\* P < 0.01, \*\*\* P < 0.001; ns, non significant difference.

**Figure 5****F508del-CFTR correction in CF-KM4 cells restored histamine ER Ca<sup>2+</sup> release compared to non CF MM39**

cells. **A** mRNA amplification of 3 isoforms of IP<sub>3</sub>R by real time PCR in MM39 and CF-KM4 cells. **B** Example of line-scan images acquired in MM39 cells and in uncorrected or corrected CF-KM4 cells in absence of extracellular Ca<sup>2+</sup>. These cells were incubated 2 h at 37°C with 100  $\mu$ M miglustat or 100  $\mu$ M NB-DGJ. **C** Average of the line-scan images in **A** expressed as normalized fluorescence in each conditions. **D** Histogram of the normalized area under curve of intensity profile of Ca<sup>2+</sup> response extracted from **A** in various experimental conditions as indicated. **E** Mean of amplitude of Ca<sup>2+</sup> response in each experimental condition. Results are presented as mean  $\pm$  SEM and the number of experiments is noted on each bar graph. \*\*\* P < 0.001; ns, non significant difference.

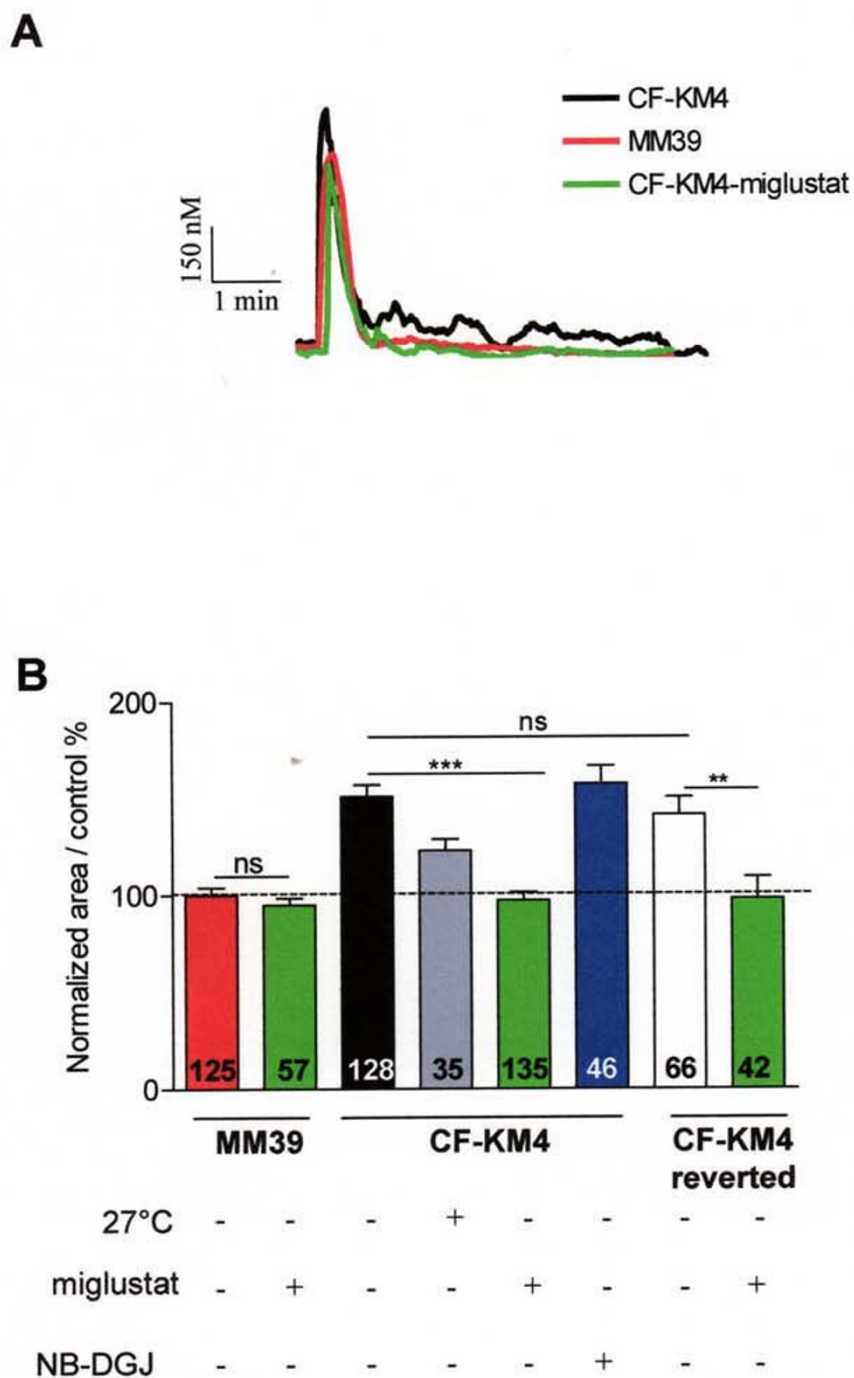


**Figure 6**  
**F508del-CFTR correction in CF-KM4 cells restored local Ca<sup>2+</sup> wave propagation compared to non CF MM39 cells.** A Typical traces of Ca<sup>2+</sup> mobilization in miglustat-treated and untreated CF-KM4 and MM39 during 5 min stimulation by 100 μM histamine in absence of extracellular Ca<sup>2+</sup>. B Histogram of the normalized area under the curve corresponding to the cytoplasmic Ca<sup>2+</sup> mobilization induced by 100 μM histamine (in 0 mM Ca<sup>2+</sup>) after various treatments. These cells were incubated 2 h at 37°C with 100 μM miglustat (for MM39, CF-KM4 and CF-KM4 reverted cells) or 24 h at 27°C, 100 μM NB-DGJ for CF-KM4 cells. The number on each bar indicates the number of cells. \*\*P < 0.01, \*\*\* P < 0.001; ns, non significant difference.

(by 25%) or miglustat (by 30%), compared to uncorrected CF-KM4 cells (Fig. 6A–B). Example tracings are performed Figure 6A. Again, these ER  $\text{Ca}^{2+}$  mobilizations are similar to that observed with MM39 cells. To emphasize the specificity of the effect of miglustat, we also noted that NB-DGJ treatment has no effect on histamine-ER  $\text{Ca}^{2+}$  release (Fig. 6B). Furthermore, the histamine-ER  $\text{Ca}^{2+}$  release in miglustat-treated MM39 cells was similar to the response observed in untreated MM39 cells (Fig. 6B). Therefore, the decrease of ER  $\text{Ca}^{2+}$  release observed in miglustat corrected CF-KM4 cells is not a side effect of miglustat on  $\text{Ca}^{2+}$  homeostasis but rather the consequence of F508del-CFTR ER escape.

#### **Direct activation of the $\text{IP}_3\text{Rs}$ using cell-permeable $\text{IP}_3$ in human tracheal gland cells**

Calcium is known to directly activate  $\text{IP}_3\text{R}$  and ryanodine receptors (RyRs), but the sensitivity of the  $\text{IP}_3$  receptors to  $\text{Ca}^{2+}$  depending on a process CICR ( $\text{Ca}^{2+}$  increase  $\text{Ca}^{2+}$  release) requires  $\text{IP}_3$  [1]. However, in absence of agonist stimulation, the level of intracellular  $\text{IP}_3$  remains very low. When we used 10 mM caffeine to activate specifically RyRs, we did not observe  $\text{Ca}^{2+}$  mobilization, on the contrary of 100  $\mu\text{M}$  histamine stimulation (Fig. 7A). These results indicate that RyRs are absent or not functional in these human epithelial cell models (CF15, CF-KM4 and MM39 cells). Then, the  $\text{Ca}^{2+}$  response produced by the NP-EGTA photolysis was the consequence of the presence and activity of  $\text{IP}_3\text{Rs}$ . This explains that the  $\text{Ca}^{2+}$  increase observed is only measured during the UV photolysis (500 ms). To eliminate these limitation of the NP-EGTA technique, and to study, more directly, the  $\text{IP}_3\text{R}$  activity, we examined the ER  $\text{Ca}^{2+}$  release by UV light photolysis of a cell-permeable caged iso-Ins(1,4,5)P3/PM in absence of extracellular  $\text{Ca}^{2+}$ . In CF-KM4 cells, preloaded with iso-Ins(1,4,5)P3/PM, short exposure (100 ms) to flash photolysis induced a biphasic increase of  $[\text{Ca}^{2+}]_i$ . We observed an initial peak of  $\text{Ca}^{2+}$  release which stabilized during 1 or 2 s, and an increase of  $\text{Ca}^{2+}$  release by a propagation of this  $\text{Ca}^{2+}$  response at the whole cell level (Fig. 7C). In MM39 and miglustat-treated CF-KM4 cells, the UV photolysis stimulated a biphasic increase of  $[\text{Ca}^{2+}]_i$ , but the amplitude of the first peak and  $\text{Ca}^{2+}$  mobilization was reduced compared to untreated CF-KM4 cells (Fig. 7C and 7D). Moreover, the second part of  $\text{Ca}^{2+}$  response was stabilized, and the rise of  $\text{Ca}^{2+}$  release was lower than the response measured for untreated CF-KM4 cells (Fig. 7C). We observed the  $[\text{Ca}^{2+}]_i$  return to a basal concentration approximately after 15 to 20 s after the UV flash (not shown). To ensure that the response evoked by exposing the cells to UV light was not due to phototoxicity or to a non-specific effect, the experiments were repeated with CF-KM4 cells loaded with fluo-4 without iso-Ins(1,4,5)P3/PM. In this experimental condition, exposure to UV flash did not induce an increase in  $[\text{Ca}^{2+}]_i$  (Fig.

7B). This experimental procedure confirms that the correction of the abnormal F508del-CFTR trafficking by miglustat induces a profound modification of  $\text{IP}_3\text{R}$   $\text{Ca}^{2+}$  dependent activity in CF cells.

#### **Consequence on $\text{IP}_3\text{Rs}$ $\text{Ca}^{2+}$ activity of F508del-CFTR ER retention in CF cells**

Finally, we used cells derived from CF-KM4 that were stably transfected to achieve low-level expression of full-length wild-type CFTR (wt-CFTR) (CF-KM4-reverted). These CF-KM4-reverted cells have been shown to have phenotypic correction of a wide range of CF phenotypes [14]. In fact, this cell line possesses both CFTR proteins: endogenous F508del-CFTR and transfected wild-type CFTR (wt-CFTR). When we measured the  $\text{Ca}^{2+}$  mobilization induced by a solution of 100  $\mu\text{M}$  histamine in absence of extracellular  $\text{Ca}^{2+}$ , this  $\text{Ca}^{2+}$  response was also similar to CF-KM4 cells (Fig. 6B). The  $\text{Ca}^{2+}$  mobilization induced by UV photolysis of iso-Ins(1,4,5)P3/PM in CF-KM4-reverted was similar to CF-KM4 cells (Fig. 7C). The plasma membrane localization of wt-CFTR did not disrupt the sensitivity of  $\text{IP}_3\text{Rs}$  to the photolysis of iso-Ins(1,4,5)P3/PM and to agonist response. To restore the endogenous F508del-CFTR trafficking, we treated these cells 2 h at 37 °C with 100  $\mu\text{M}$  miglustat. In this condition, the specific  $\text{IP}_3\text{R}$  activity, measured by  $\text{Ca}^{2+}$  response to agonist stimulation and by iso-Ins(1,4,5)P3/PM photolysis was reduced to the level measured in non CF cells (Fig. 6B and 7C). This abnormal increase of  $\text{IP}_3\text{R}$   $\text{Ca}^{2+}$  release in CF human epithelial cells compared to non CF cells appear thus to be the consequence of F508del-CFTR retention in ER compartment.

#### **Morphology of the ER in non CF and CF cells**

To begin to understand the cause of the ER  $\text{Ca}^{2+}$  release abnormal in CF cells, we examined the ER morphology in our experimental conditions. In a first set of experiments, the ER structure was investigated by calreticulin immunofluorescence (Fig. 8A). Calreticulin is an intraluminal ER protein involved in  $\text{Ca}^{2+}$  sequestration [21]. Figure 8A shows that the ER remains highly concentrated around the nucleus in untreated or NB-DGJ-treated CF-KM4 cells. On the contrary, in MM39 and in miglustat-corrected-CF-KM4 cells, the ER is spreaded throughout the cells. No immunostaining of calreticulin was detected when the primary antibodies were omitted (data not shown). To verify whether this difference in ER morphology observed between CF and non CF cells is due to the ER structure or to a change of calreticulin localization, we also stained the ER with a specific fluorescent probes (ER tracker) (Fig. 8B). Again, the ER was also found highly concentrated around the nucleus in untreated and NB-DGJ-treated CF-KM4 cells, whereas in periphery of the cells the ER network was very thin. On the contrary, in non CF cells or corrected CF cells, the ER was clearly extended throughout

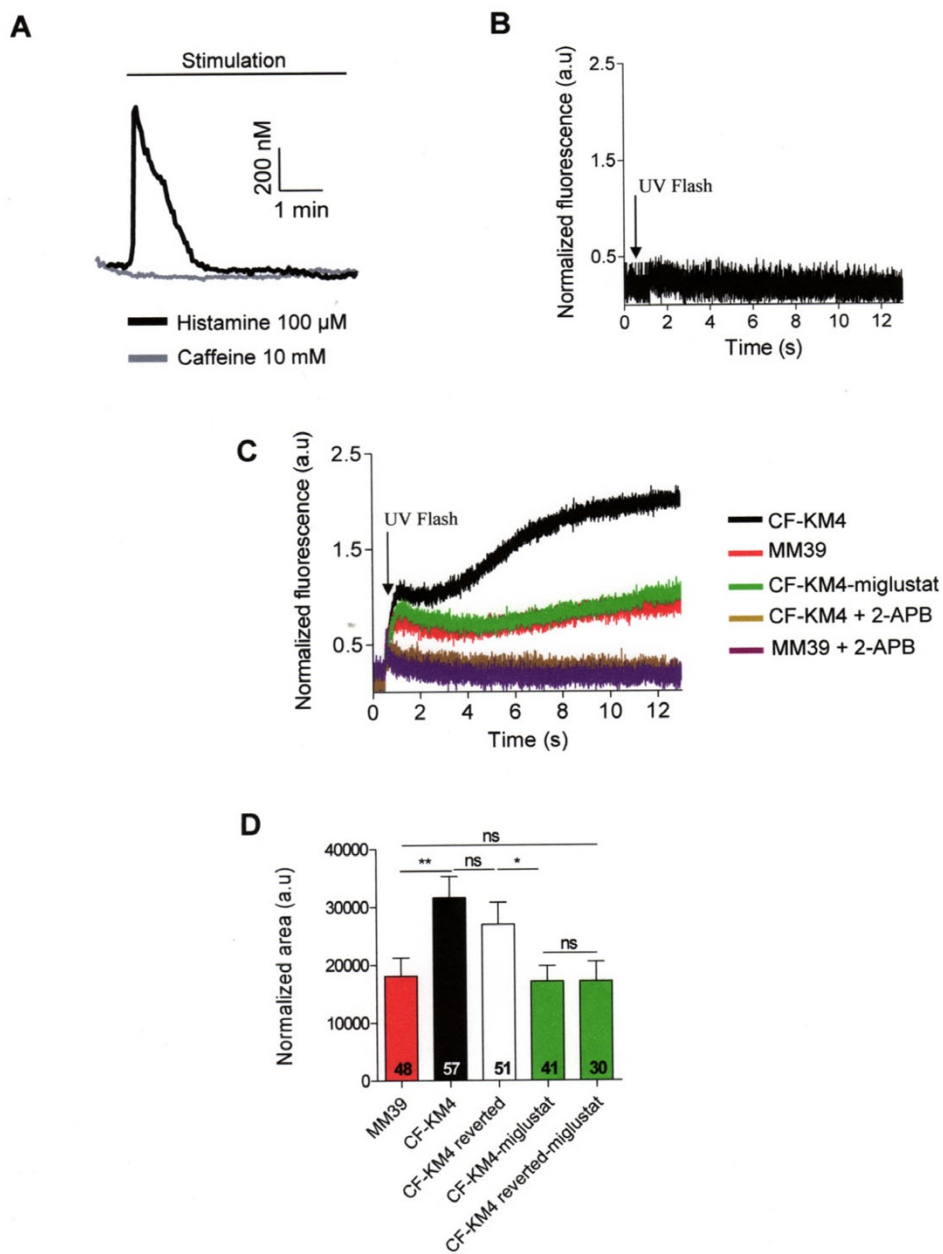


**Figure 7**

**Flash photolysis of iso-Ins(1,4,5)P3/PM induced release from internal stores in human tracheal gland cells.** **A** Typical traces of Ca<sup>2+</sup> mobilization in CF-KM4 cells during 5 min stimulation by 100  $\mu$ M histamine or 10 mM caffeine in absence of extracellular Ca<sup>2+</sup>. **B** The CF-KM4 cells were loaded with fluo-4 and without iso-Ins(1,4,5)P3/PM and stimulated by UV light. **C** Traces show average normalized fluo4 fluorescence recordings in uncorrected or corrected CF-KM4 (incubated 2 h at 37°C with 100  $\mu$ M miglustat) and in MM39 cells in absence of extracellular Ca<sup>2+</sup>. These cells were preincubated during 10 min in presence or not of 100  $\mu$ M 2-APB. **D** Histogram of the normalized area under curve of intensity profile of Ca<sup>2+</sup> response in various experimental conditions as indicated. These cells were incubated 2 h at 37°C with 100  $\mu$ M miglustat (CF-KM4 and CF-KM4 reverted cells). Results are presented as mean  $\pm$  SEM and the number of experiments is noted on each bar graph. \* P < 0.05; \*\* P < 0.01; \*\*\* P < 0.001; ns, non significant difference.

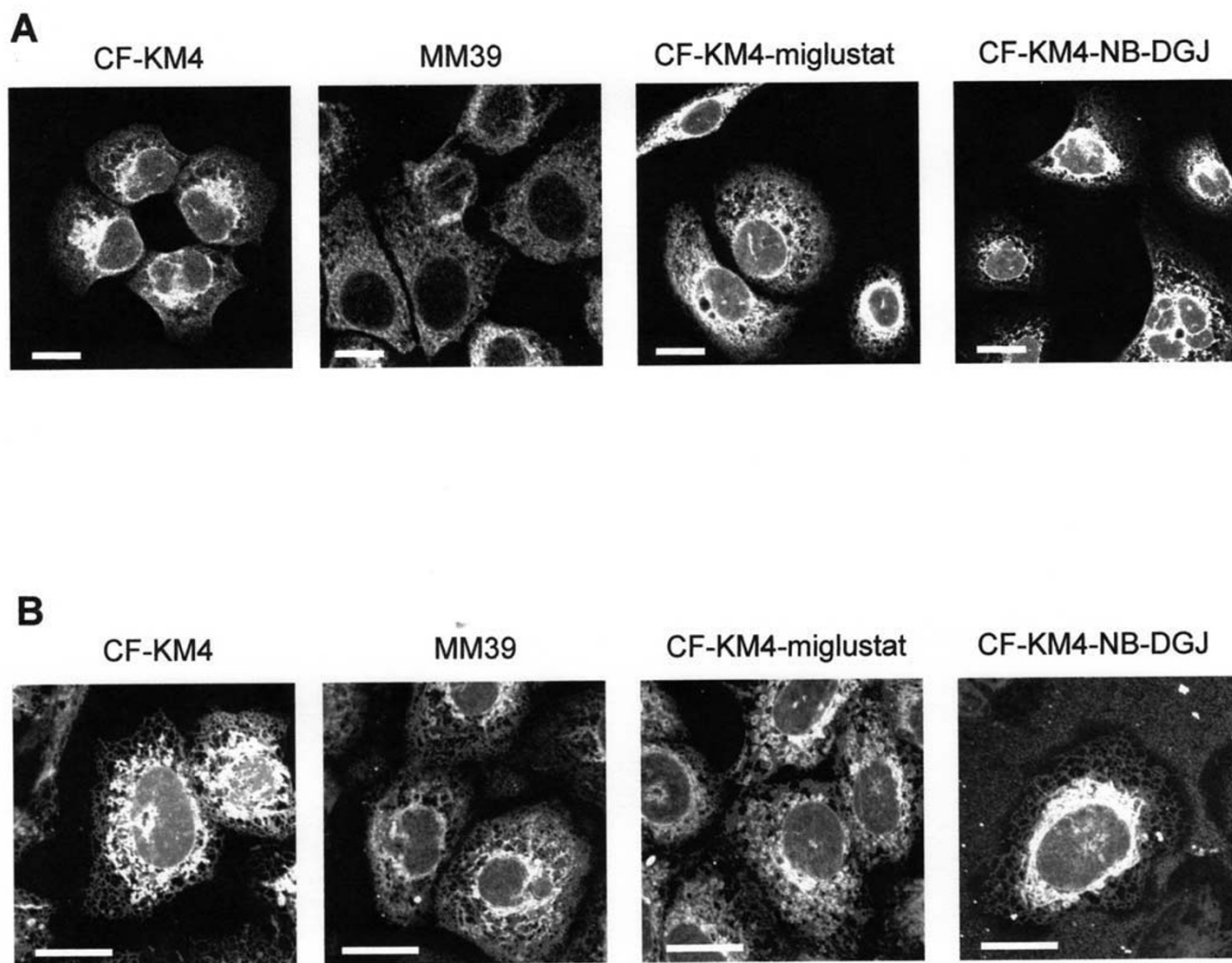


**Figure 8**  
**ER morphology in uncorrected or corrected CF human tracheal gland cells compared to non CF human tracheal gland cells.** A Immunostaining of calreticulin in untreated CF-KM4, MM39 and miglustat (100  $\mu$ M 2 h) or NB-DGJ (100  $\mu$ M 2 h) treated CF-KM4 cells. Nuclei are labelled with TOPRO-3, bar = 10  $\mu$ m. B ER imaging (with ER tracker probes) in untreated or miglustat (100  $\mu$ M 2 h) or NB-DGJ (100  $\mu$ M 2 h) treated CF-KM4 cells and in untreated MM39 cells, bar = 10  $\mu$ m.

the cell (Fig. 8B). Thus treatment of CF cells with the corrector miglustat induces an ER spreading throughout the cells.

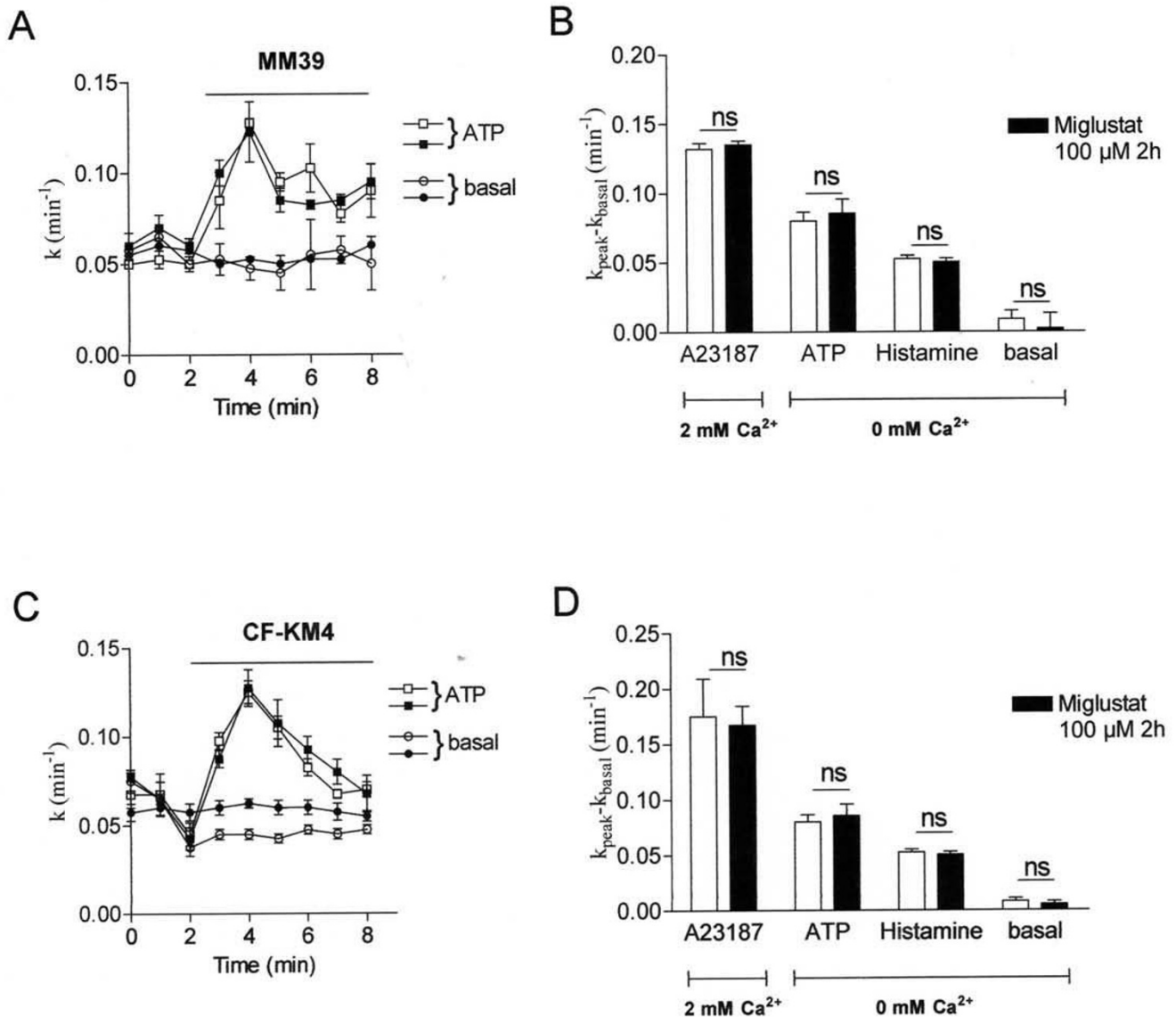
**What is the consequence of the ER  $Ca^{2+}$  decreased on the CaCC activity?**

Since intracellular  $Ca^{2+}$  regulates the functionality of numerous proteins and because the ER  $Ca^{2+}$  mobilization was decreased in miglustat-CF cells, we determined whether these changes in  $Ca^{2+}$  signalling lead to changes in the  $Ca^{2+}$  mediated  $Cl^{-}$  transport. The  $Ca^{2+}$ -activated  $Cl^{-}$  channels (CaCC) are functionally expressed in many non excitable cells [22,23]. We performed iodide efflux experiments in untreated and miglustat-treated MM39 (Fig. 9A)

and CF-KM4 (Fig. 9B) cells and stimulated the activity of CaCC by the  $Ca^{2+}$  ionophore A23187. No variation was detected following the treatment of cells by miglustat (Fig. 9). Then we examined the activity of CaCC stimulated by ER  $Ca^{2+}$  release using two different agonists (ATP and histamine). Again no difference was observed between untreated vs miglustat treated cells. Taken altogether, and in spite of the decreased ER  $Ca^{2+}$  mobilization in miglustat-corrected-CF cells, the activity of CaCC remained unaffected by miglustat.

**Discussion**

Our study on the regulation of  $Ca^{2+}$  signalling in human F508del-CFTR and in corrected CF cells reveals that (i) the

**Figure 9**

**ER Ca<sup>2+</sup> release decreased after F508del-CFTR correction, what is the consequence on calcium-activated chloride channel (CaCC) activity?** A Example of mean iodide efflux for activation of CaCC in miglustat-treated (black symbol) or not (open symbol) MM39 cells. CaCC were stimulated by 100 μM ATP in 0 mM Ca<sup>2+</sup> bath medium. B Histograms show the mean relative rate for the experimental conditions (1 μM A23187, 100 μM ATP or 100 μM histamine) indicated below each bar (n = 4) in miglustat-treated (black bars) or not (open bars) MM39 cells. C Examples of mean iodide efflux for activation of CaCC in miglustat-treated (black symbol) or not (open symbol) CF-KM4 cells. CaCC were stimulated as for MM39 cells. D Histograms show the mean relative rate for the experimental conditions indicated below each bar (n = 4) in miglustat-treated (black bars) or not (open bars) CF-KM4 cells. Results are presented as mean ± S.E.M; ns, non significant difference.

release of ER Ca<sup>2+</sup> store is dependent on the presence of the three isoforms of IP<sub>3</sub>R, (ii) the activity of IP<sub>3</sub>R is implicated in the propagation of Ca<sup>2+</sup> waves (iii) correction of the abnormal trafficking of F508del-CFTR in CF cells regulates local ER Ca<sup>2+</sup> release which is correlated to

a normalization of this local ER Ca<sup>2+</sup> mobilization, (iv) IP<sub>3</sub>R1 participation in Ca<sup>2+</sup> response is decreased in corrected CF15 cells (v) the ER was spreaded throughout the cells, i.e. non CF or corrected CF cells compared to uncorrected CF cells where the ER was condensed around

nucleus, (vi) the activity of  $\text{Ca}^{2+}$ -dependent  $\text{Cl}^-$  channels are not affected in CF cells, non CF cells, or corrected CF cells.

We propose that  $\text{Ca}^{2+}$  homeostasis in cystic fibrosis airway epithelial cells is disturbed and related to the retention in the ER of F508del-CFTR proteins.

Epithelium from trachea to distal intrapulmonary airways (bronchioles) presented positive immunoreactivity for all types of  $\text{IP}_3\text{Rs}$  [24]. All three isoforms of  $\text{IP}_3\text{Rs}$  are also expressed in Madin-Darby canine kidney cells, a well studied tight polarized epithelial cell type [25]. Thus, in epithelial cell models, multiple isoforms of  $\text{IP}_3\text{R}$  appeared to be present in a single cell. In our epithelial models, we showed the presence of the three isoforms. In CF15 cells their localisation is comparable, *i.e.* diffuse in the cytoplasm of the cells. Moreover, no variation of  $\text{IP}_3\text{Rs}$  mRNA was observed. The three subtypes of  $\text{IP}_3\text{R}$   $\text{Ca}^{2+}$  release channels share basic properties but differ in term of regulation. Type 1  $\text{IP}_3\text{R}$ , with both  $\text{Ca}^{2+}$ -dependent activation and inhibition, is well suited for establishing  $\text{Ca}^{2+}$  oscillations [1,26,27], where the frequency of  $\text{Ca}^{2+}$  transients can be modulated when  $\text{IP}_3$  concentrations are increased [27,28]. The effects of CsA are lower in CF15 corrected cells than in uncorrected CF15 cells; it suggests that the CsA-sensitive  $\text{IP}_3\text{R}$  participation in  $\text{Ca}^{2+}$  response was decreased in CF15 corrected cells.

Human CF primary bronchial epithelial cells and respiratory cell lines were reported to produce an exaggerated proinflammatory cytokine response associated with an activation of  $\text{NF-}\kappa\text{B}$  [29-31]. Intracellular  $\text{Ca}^{2+}$  is known to play a central role in production and secretion of  $\text{IL-8}$  [32,33]. The  $\text{IL-1}\beta$  stimulation induces a prolonged  $[\text{Ca}^{2+}]_i$  in IB3-1 cells which was correlated to  $\text{NF-}\kappa\text{B}$  activation [34]. The deregulation of  $\text{IP}_3\text{R}$   $\text{Ca}^{2+}$  release observed in human nasal and tracheal epithelial cells could be implicated in increasing inflammatory response observed in numerous CF cell lines in particular in CF epithelial cells [6,34].

The apical ER network is expended in human CF bronchial epithelial cells compared to ER volume in human non CF bronchial epithelial cells [6]. In this present study, the ER staining (by calreticulin immunostaining or ER tracker probe) shows that the ER structure is highly different in CF compared to non CF or CF-corrected cells. The ER volume seems to be concentrated around the nucleus in CF cells and expanded throughout the cytoplasm of non CF and CF-corrected cells. This expansion could be responsible for the variation in  $\text{IP}_3\text{R}$   $\text{Ca}^{2+}$  dependent activity observed in this present study. Indeed, the display of ER web could induce probably an augmentation of distance between  $\text{IP}_3$  receptors which would induce a

decrease in the propagation of the  $\text{Ca}^{2+}$  response. Furthermore, the F508del-CFTR correction is causing a potential redistribution of  $\text{IP}_3\text{Rs}$  at the ER membrane. We believed that in corrected CF and non CF cells,  $\text{IP}_3\text{Rs}$  are more distant from each others, leading to reduce propagation of the  $\text{Ca}^{2+}$  wave. Then  $\text{IP}_3\text{Rs}$  clustering of the ER could facilitate the formation of highly sensitive  $\text{Ca}^{2+}$  release sites, thereby stimulating the  $\text{Ca}^{2+}$  wave initiation and propagation [35]. For example, in maturation of oocytes, the modifications in ER clusters are accompanied by an increase in the sensitivity of  $\text{Ca}^{2+}$  release by  $\text{IP}_3$  [36,37]. Moreover, in CF cells  $\text{IP}_3\text{Rs}$  are closer to each other and the photolysis induces a long  $\text{Ca}^{2+}$  wave due to a better propagation. Our interpretation of the data obtained with CF-KM4-reverted cells is that the  $\text{IP}_3\text{Rs}$  deregulation is not due to the CFTR absence at the plasma membrane but is more likely due to the abnormal ER F508del-CFTR retention. The F508del-CFTR escape of ER by pharmacological corrector treatment induces the normalization of  $\text{IP}_3\text{R}$   $\text{Ca}^{2+}$  release.

In the airways, pleiotropic consequences accompanied the production of F508del-CFTR protein generating vicious cycle of airway obstruction, infection, and inflammation at the origin of most of the morbidity and mortality in cystic fibrosis. The pro-inflammatory mediator bradykinin triggers  $\text{Ca}^{2+}$  mobilization [38,39] and induces interleukin-8 secretion in non-CF and CF human airway epithelia [40,41]. A mechanism has been proposed to explain the increase of  $\text{Ca}^{2+}$  signals at the apical membrane in human CF airway epithelia; it results from the expansion of the ER  $\text{Ca}^{2+}$  store compartment rather than from a greater number of purinergic receptors [6,40]. We can confirm these results in our cellular models because we observed that the kinetics of activation of the  $\text{Ca}^{2+}$  response obtained in NB-DNJ-treated CF cells do not mimic the effect of the inhibitors of the  $\text{IP}_3\text{R}$  and we observed a variation of the ER morphology between non CF or corrected and uncorrected epithelial cells.

We recently provided evidence that the pharmacological correction of abnormal trafficking of F508del-CFTR [12] induces a restoration of  $\text{Ca}^{2+}$  mobilization in CF cells [5]. Here, we showed reduction of the inositol 1,4,5-trisphosphate receptors ( $\text{IP}_3\text{R}$ ) dependent- $\text{Ca}^{2+}$  response following two different correcting treatments compared to uncorrected cells in such a way that  $\text{Ca}^{2+}$  responses (CF+treatment *vs* wild-type cells) were normalized. Altogether, these results suggest reversal of the  $\text{IP}_3\text{R}$  dysfunction in F508del-CFTR epithelial cells by a pharmacological correction of the abnormal trafficking of F508del-CFTR in cystic fibrosis cells.

## Abbreviations list

AM: Acetoxymethyl; 2-APB: 2-aminoethoxydiphenyl borate; CF: cystic fibrosis; CFTR: cystic fibrosis transmembrane conductance regulator; ER: endoplasmic reticulum; IP<sub>3</sub>: inositol 1,4,5-trisphosphate; IP<sub>3</sub> caged: iso-Ins(1,4,5)P<sub>3</sub>/PM; IP<sub>3</sub>R: IP<sub>3</sub> receptor; NB-DGJ: N-butyldeoxygalactojirimycin; NB-DNJ: N-butyldeoxynojirimycin; NP-EGTA: Nitrophenyl-Ethylene Glycol-bis(β-Aminoethyl ether) N,N,N',N'-Tetraacetic Acid; TG: Thapsigargin; CsA: Cyclosporine A.

## Competing interests

The authors declare that they have no competing interests.

## Authors' contributions

FA conducted the experiments, analysed the data and wrote the draft of the manuscript. CN realized the iodide efflux experiments. AC helped us to realized confocal microscopy experiments and analysis. FB and CV revised the manuscript. All authors read and approved of the final manuscript.

## Acknowledgements

The authors thank Nathalie Bizard, Dr. Sylvie Patri, and Dr. Vincent Thoreau for expert technical assistance. This work was supported by Vaincre la Mucoviscidose (VLM) and CNRS. Fabrice Antigny and Caroline Norez were supported by a studentship from VLM. The authors thank Dr. Christelle Coraux for the generous gift of the CF-KM4-reverted cell line.

## References

- Bezprozvanny I, Watras J, Ehrlich BE: **Bell-shaped calcium-response curves of Ins(1,4,5)P<sub>3</sub>- and calcium-gated channels from endoplasmic reticulum of cerebellum.** *Nature* 1991, **351**:751-754.
- De Smedt H, Missiaen L, Parys JB, Henning RH, Sienaert I, Vanlingen S, et al.: **Isoform diversity of the inositol trisphosphate receptor in cell types of mouse origin.** *Biochem J* 1997, **322**(Pt 2):575-583.
- Thrower EC, Hagar RE, Ehrlich BE: **Regulation of Ins(1,4,5)P<sub>3</sub> receptor isoforms by endogenous modulators.** *Trends Pharmacol Sci* 2001, **22**:580-586.
- Hagar RE, Burgstahler AD, Nathanson MH, Ehrlich BE: **Type III InsP<sub>3</sub> receptor channel stays open in the presence of increased calcium.** *Nature* 1998, **396**:81-84.
- Antigny F, Norez C, Becq F, Vandebrouck C: **Calcium homeostasis is abnormal in cystic fibrosis airway epithelial cells but is normalized after rescue of F508del-CFTR.** *Cell Calcium* 2008, **43**:175-183.
- Ribeiro CM, Paradiso AM, Carew MA, Shears SB, Boucher RC: **Cystic fibrosis airway epithelial Ca<sup>2+</sup> signaling: the mechanism for the larger agonist-mediated Ca<sup>2+</sup> signals in human cystic fibrosis airway epithelia.** *J Biol Chem* 2005, **280**:10202-10209.
- Pind S, Riordan JR, Williams DB: **Participation of the endoplasmic reticulum chaperone calnexin (p88, IP90) in the biogenesis of the cystic fibrosis transmembrane conductance regulator.** *J Biol Chem* 1994, **269**:12784-12788.
- Cheng SH, Gregory RJ, Marshall J, Paul S, Souza DW, White GA, et al.: **Defective intracellular transport and processing of CFTR is the molecular basis of most cystic fibrosis.** *Cell* 1990, **63**:827-834.
- Jefferson DM, Valentini JD, Marini FC, Grubman SA, Iannuzzi MC, Dorkin HL, et al.: **Expression of normal and cystic fibrosis phenotypes by continuous airway epithelial cell lines.** *Am J Physiol* 1990, **259**:L496-L505.
- Kammouni W, Moreau B, Becq F, Saleh A, Pavirani A, Figarella C, et al.: **A cystic fibrosis tracheal gland cell line, CF-KM4. Correction by adenovirus-mediated CFTR gene transfer.** *Am J Respir Cell Mol Biol* 1999, **20**:684-691.
- Merten MD, Kammouni W, Renaud W, Birg F, Mattei MG, Figarella C: **A transformed human tracheal gland cell line, MM-39, that retains serous secretory functions.** *Am J Respir Cell Mol Biol* 1996, **15**:520-528.
- Norez C, Noel S, Wilke M, Bijvelde M, Jorna H, Melin P, et al.: **Rescue of functional delF508-CFTR channels in cystic fibrosis epithelial cells by the alpha-glucosidase inhibitor miglustat.** *FEBS Lett* 2006, **580**:2081-2086.
- Denning GM, Anderson MP, Amara JF, Marshall J, Smith AE, Welsh MJ: **Processing of mutant cystic fibrosis transmembrane conductance regulator is temperature-sensitive.** *Nature* 1992, **358**:761-764.
- Bacconnais S, Delavoie F, Zahm JM, Milliot M, Terryn C, Castillon N, et al.: **Abnormal ion content, hydration and granule expansion of the secretory granules from cystic fibrosis airway glandular cells.** *Exp Cell Res* 2005, **309**:296-304.
- Auzanneau C, Thoreau V, Kitzis A, Becq F: **A Novel voltage-dependent chloride current activated by extracellular acidic pH in cultured rat Sertoli cells.** *J Biol Chem* 2003, **278**:19230-19236.
- Norez C, Antigny F, Becq F, Vandebrouck C: **Maintaining low Ca<sup>2+</sup> level in the endoplasmic reticulum restores abnormal endogenous F508del-CFTR trafficking in airway epithelial cells.** *Traffic* 2006, **7**:562-573.
- Ellis-Davies GC, Kaplan JH: **Nitrophenyl-EGTA, a photolabile chelator that selectively binds Ca<sup>2+</sup> with high affinity and releases it rapidly upon photolysis.** *Proc Natl Acad Sci USA* 1994, **91**:187-191.
- Bultynck G, Sienaert I, Parys JB, Callewaert G, De Smedt H, Boens N, et al.: **Pharmacology of inositol trisphosphate receptors.** *Pflugers Arch* 2003, **445**:629-642.
- Maes K, Missiaen L, De Smet P, Vanlingen S, Callewaert G, Parys JB, et al.: **Differential modulation of inositol 1,4,5-trisphosphate receptor type I and type 3 by ATP.** *Cell Calcium* 2000, **27**:257-267.
- Genazzani AA, Carafoli E, Guerini D: **Calcineurin controls inositol 1,4,5-trisphosphate type I receptor expression in neurons.** *Proc Natl Acad Sci USA* 1999, **96**:5797-5801.
- Michalak M, Mariani P, Opas M: **Calreticulin, a multifunctional Ca<sup>2+</sup> binding chaperone of the endoplasmic reticulum.** *Biochem Cell Biol* 1998, **76**:779-785.
- Arreola J, Melvin JE, Begenisich T: **Activation of calcium-dependent chloride channels in rat parotid acinar cells.** *J Gen Physiol* 1996, **108**:35-47.
- Jentsch TJ: **Chloride channels: a molecular perspective.** *Curr Opin Neurobiol* 1996, **6**:303-310.
- Sugiyama T, Yamamoto-Hino M, Wasano K, Mikoshiba K, Hasegawa M: **Subtype-specific expression patterns of inositol 1,4,5-trisphosphate receptors in rat airway epithelial cells.** *J Histochem Cytochem* 1996, **44**:1237-1242.
- Bush KT, Stuart RO, Li SH, Moura LA, Sharp AH, Ross CA, et al.: **Epithelial inositol 1,4,5-trisphosphate receptors. Multiplicity of localization, solubility, and isoforms.** *J Biol Chem* 1994, **269**:23694-23699.
- Dixon CJ, Woods NM, Cuthbertson KS, Cobbold PH: **Evidence for two Ca<sup>2+</sup>-mobilizing purinoceptors on rat hepatocytes.** *Biochem J* 1990, **269**:499-502.
- Petersen CC, Toescu EC, Potter BV, Petersen OH: **Inositol triphosphate produces different patterns of cytoplasmic Ca<sup>2+</sup> spiking depending on its concentration.** *FEBS Lett* 1991, **293**:179-182.
- Kaftan EJ, Ehrlich BE, Watras J: **Inositol 1,4,5-trisphosphate (InsP<sub>3</sub>) and calcium interact to increase the dynamic range of InsP<sub>3</sub> receptor-dependent calcium signaling.** *J Gen Physiol* 1997, **110**:529-538.
- Tabary O, Escotte S, Couetil JP, Hubert D, Dusser D, Puchelle E, et al.: **Genistein inhibits constitutive and inducible NFκB activation and decreases IL-8 production by human cystic fibrosis bronchial gland cells.** *Am J Pathol* 1999, **155**:473-481.
- Venkatakrishnan A, Stecenko AA, King G, Blackwell TR, Brigham KL, Christman JW, et al.: **Exaggerated activation of nuclear factor-κB and altered IκBβ processing in cystic fibro-**

- sis bronchial epithelial cells. *Am J Respir Cell Mol Biol* 2000, **23**:396-403.
31. Weber AJ, Soong G, Bryan R, Saba S, Prince A: **Activation of NF-kappaB in airway epithelial cells is dependent on CFTR trafficking and Cl-channel function.** *Am J Physiol Lung Cell Mol Physiol* 2001, **281**:L71-L78.
  32. Kuhns DB, Young HA, Gallin EK, Gallin JI: **Ca<sup>2+</sup>-dependent production and release of IL-8 in human neutrophils.** *J Immunol* 1998, **161**:4332-4339.
  33. Marino F, Cosentino M, Fietta AM, Ferrari M, Cattaneo S, Frigo G, et al.: **Interleukin-8 production induced by the endozepine triakontatetrauropeptide in human neutrophils: role of calcium and pharmacological investigation of signal transduction pathways.** *Cell Signal* 2003, **15**:511-517.
  34. Tabary O, Boncoeur E, de Martin R, Pepperkok R, Clement A, Schultz C, et al.: **Calcium-dependent regulation of NF-(kappa)B activation in cystic fibrosis airway epithelial cells.** *Cell Signal* 2006, **18**:652-660.
  35. Swillens S, Dupont G, Combettes L, Champeil P: **From calcium blips to calcium puffs: theoretical analysis of the requirements for interchannel communication.** *Proc Natl Acad Sci USA* 1999, **96**:13750-13755.
  36. Kume S, Muto A, Aruga J, Nakagawa T, Michikawa T, Furuichi T, et al.: **The Xenopus IP3 receptor: structure, function, and localization in oocytes and eggs.** *Cell* 1993, **73**:555-570.
  37. Vermassen E, Parys JB, Mauger JP: **Subcellular distribution of the inositol 1,4,5-trisphosphate receptors: functional relevance and molecular determinants.** *Biol Cell* 2004, **96**:3-17.
  38. Paradiso AM, Cheng EH, Boucher RC: **Effects of bradykinin on intracellular calcium regulation in human ciliated airway epithelium.** *Am J Physiol* 1991, **261**:L63-L69.
  39. Kotlikoff MI, Murray RK, Reynolds EE: **Histamine-induced calcium release and phorbol antagonism in cultured airway smooth muscle cells.** *Am J Physiol* 1987, **253**:C561-C566.
  40. Ribeiro CM, Paradiso AM, Schwab U, Perez-Vilar J, Jones L, O'neal W, et al.: **Chronic airway infection/inflammation induces a Ca<sup>2+</sup>-dependent hyperinflammatory response in human cystic fibrosis airway epithelia.** *J Biol Chem* 2005, **280**:17798-17806.
  41. Rodgers HC, Pang L, Holland E, Corbett L, Range S, Knox AJ: **Bradykinin increases IL-8 generation in airway epithelial cells via COX-2-derived prostanoids.** *Am J Physiol Lung Cell Mol Physiol* 2002, **283**:L612-L618.

Publish with **BioMed Central** and every scientist can read your work free of charge

"BioMed Central will be the most significant development for disseminating the results of biomedical research in our lifetime."

Sir Paul Nurse, Cancer Research UK

Your research papers will be:

- available free of charge to the entire biomedical community
- peer reviewed and published immediately upon acceptance
- cited in PubMed and archived on PubMed Central
- yours — you keep the copyright

Submit your manuscript here:  
[http://www.biomedcentral.com/info/publishing\\_adv.asp](http://www.biomedcentral.com/info/publishing_adv.asp)

